GEOPHYSICAL RESEARCH LETTERS, VOL. 40, 5003–5008, doi:10.1002/grl.50979, 2013

Magnetospheric "magic" frequencies as magnetopause surface eigenmodes

M. O. Archer,[1] M. D. Hartinger,[2] and T. S. Horbury[1]

Received 5 September 2013; revised 19 September 2013; accepted 20 September 2013; published 4 October 2013.

[1] The persistent so-called "magic" magnetospheric frequencies are thought to be either directly driven by monochromatic solar wind pressure fluctuations or resonantly excited global (cavity/waveguide) or magnetopause surface eigenmodes. We distinguish between these cases by statistically investigating, using simultaneous observations, the magnetospheric response to jets in the subsolar magnetosheath. The broadband jets do not exhibit discrete frequencies but do drive waves at the discrete magic frequencies, with both direct and resonant driving. We show that the expected fundamental frequencies of magnetopause surface eigenmodes have two preferential values over a wide range of upstream conditions, corresponding to fast and slow solar wind, and that their harmonics are in good agreement with the magic frequencies. We also show that the waves are largely inconsistent with global modes outside the plasmasphere. Thus, we conclude that these magic frequencies are most likely due to magnetopause surface eigenmodes.
Citation: Archer, M. O., M. D. Hartinger, and T. S. Horbury (2013), Magnetospheric "magic" frequencies as magnetopause surface eigenmodes, *Geophys. Res. Lett.*, *40*, 5003–5008, doi:10.1002/grl.50979.

1. Introduction

[2] Statistical and event studies have shown that magnetospheric ultralow frequency (ULF) waves are often observed at persistent discrete frequencies (roughly 0.7, 1.3, 1.9, 2.6, 3.3, and 4.8 mHz) known as "magic" frequencies (see *Menk* [2011] for a recent review), first seen in high-latitude ionospheric radar measurements [*Samson et al.*, 1992] and ground-based magnetometer data [*Francia and Villante*, 1997]. Due to their perseverance and the regularity of the sequence, it has been suggested that the magic frequencies are eigenfrequencies of the magnetospheric system with a fundamental frequency ∼0.65 mHz and are often assumed to be either cavity or waveguide modes, radially standing fast mode waves trapped between magnetospheric boundaries [e.g., *Kivelson and Southwood*, 1985; *Samson et al.*, 1992], which we refer to here as global modes. These modes are expected to have a 90° phase difference between the compressional magnetic field and azimuthal electric field perturbations, along with nodes and antinodes in their radial profiles (especially in the harmonics) [*Waters et al.*, 2002]. However, some theoretical [e.g., *Lee and Lysak*, 1989] and observational [e.g., *Hartinger et al.*, 2013] studies have shown that the frequencies of global modes outside the plasmasphere are typically higher than the magic values.

[3] *Kepko et al.* [2002] and *Kepko and Spence* [2003] showed simultaneous observations of highly correlated, monochromatic solar wind density and magnetospheric magnetic field fluctuations at the magic frequencies. They argued that rather than being inherent to the magnetosphere, these frequencies are due to typical length scales in the solar wind driving waves directly. Indeed, *Viall et al.* [2009] reported that the magic frequencies are observed in the magnetosphere 54% of the time that they occur in the solar wind.

[4] Finally, *Plaschke et al.* [2009] proposed that the magic frequencies are eigenmodes of standing Alfvénic magnetopause surface waves due to the prominence of these frequencies in observations of the oscillating boundary as well as a fundamental frequency estimate using typical conditions. Such surface waves should have an evanescent wave component inside the magnetosphere. Under this framework, however, it is not clear why the magic frequencies are so stable over a wide range of upstream conditions. It has been suggested that localized pressure enhancements in the magnetosheath may be able to excite such modes [*Plaschke and Glassmeier*, 2011].

[5] In this paper we distinguish between these three hypotheses for the magic frequencies by testing their predictions during intervals of magnetosheath jets (also known as dynamic pressure pulses/enhancements). Such jets occur around 2% of the time, predominantly downstream of the quasi-parallel shock, and have dimensions ∼0.2–0.5 R_E perpendicular to the flow, durations of around 30 s on average, and amplitudes of up to ∼15 times the ambient dynamic pressure (principally due to velocity increases) and ∼2 times the ambient total pressure [*Archer et al.*, 2012; *Archer and Horbury*, 2013]. It is known that these broadband structures can perturb the boundary [e.g., *Shue et al.*, 2009] and excite Pc5–6 (below 7 mHz) waves in the magnetosphere [*Archer et al.*, 2013, henceforth called A13]. Thus, these structures can be used to test the surface eigenmode interpretation of the magic frequencies against the other hypotheses. Such a study requires measurements of both the specific driver (the jets) and response, thus simultaneous observations in the magnetosheath and magnetosphere are key.

2. Method

2.1. Event Selection

[6] In this study we use observations of magnetosheath jets by Time History of Events and Macroscale Interactions

Additional supporting information may be found in the online version of this article.

[1]Space and Atmospheric Physics Group, The Blackett Laboratory, Imperial College London, London, UK.
[2]Department of Atmospheric, Oceanic and Space Sciences, University of Michigan, Ann Arbor, Michigan, USA.

Corresponding author: M. O. Archer, Space and Atmospheric Physics Group, The Blackett Laboratory, Imperial College London, Prince Consort Rd., London SW7 2AZ, UK. (m.archer10@imperial.ac.uk)

0094-8276/13/10.1002/grl.50979

during Substorms (THEMIS) [*Angelopoulos*, 2008], identified by *Archer and Horbury* [2013], and the magnetospheric response at GOES. We select only events which satisfy the following criteria:

[7] 1. Focusing on the subsolar region, we require both a THEMIS and GOES spacecraft between 10:30 and 13:30 magnetic local time (MLT). If more than one GOES spacecraft satisfied this criterion for an event, the one closest to 12:00 MLT was chosen.

[8] 2. For the 2 h interval centered on the jet, the THEMIS spacecraft must have been solely in the magnetosheath, allowing simultaneous measurements of the drive (jets) and response (by GOES) at Pc5–6 frequencies, which can be difficult to observe.

[9] 3. One minute resolution solar wind data, lagged to the bow shock nose, from the OMNI database were required to control for upstream conditions.

[10] 4. In order for the jet to constitute a significant pressure increase, the amplitude of the dynamic pressure enhancement had to be greater than 20% of the background total pressure (dynamic + ion thermal + magnetic) calculated using THEMIS electrostatic analyzer (ESA) [*McFadden et al.*, 2008a] and fluxgate magnetometer (FGM) [*Auster et al.*, 2008].

[11] This yielded 130 events (see the supporting information for times) and we also randomly picked the same number of (null) events at random satisfying criteria 1–3. GOES magnetometer data were transformed into a coordinate system with field-aligned/compressional component **F**, azimuthal/toroidal component **A**, and radial/poloidal component **R**.

2.2. Estimating Field Line Resonance Frequencies

[12] To distinguish between global and local effects, we estimate the fundamental frequencies f_{FLR} of field line resonances (FLRs) [e.g., *Southwood*, 1974] at the GOES spacecraft for each event using the time of flight approximation and T96 model [*Tsyganenko*, 1995; *Tsyganenko and Stern*, 1996] as detailed by A13. However, GOES has no instrument to measure the equatorial density of the cold magnetospheric plasma required in this calculation. Therefore, we take the (20 min averaged) spacecraft potential inferred density [*McFadden et al.*, 2008b] from whichever of the five THEMIS spacecraft crossings of geostationary orbit (within 08:00-16:00 MLT) was temporally nearest, assuming the density did not change significantly over the time difference between these two observations (which peaked 20 min before the jet with a standard deviation of $2\frac{3}{4}$ h). The calculations resulted in frequencies (highly correlated with the observed density) with two main populations:

[13] 1. $f_{\mathrm{FLR}} > 10$ mHz corresponding to densities 0.5–10 cm^{-3} (77 events)

[14] 2. $f_{\mathrm{FLR}} < 10$ mHz corresponding to densities 50–1500 cm^{-3} (53 events)

[15] In this study we only require that the FLR frequencies are broadly correct and estimate through sensitivity tests that they are accurate to ∼15%. To better understand these two populations in terms of the magnetospheric configuration, we take THEMIS-A's nearest magnetosphere crossing (since it has the shortest orbital period ∼21 h) for each event and bin density observations by L shell. The median density profiles for the two f_{FLR} cases are shown in Figure 1 (top) with all crossings in the insets to show the level of variability. For high f_{FLR} cases, the plasmapause is typically well defined (the sharp jumps in density seen in the inset) and at a lower L shell than geostationary orbit. In contrast, low f_{FLR} cases show a smooth transition between magnetospheric and plasmaspheric densities, similar to those reported during quiet times by *Tu et al.* [2007]. We also estimate the Alfvén speed and FLR frequency profiles using the T96 model. The high f_{FLR} cases yielded results consistent with previous modeling [e.g., *Lee and Lysak*, 1989], whereas the low f_{FLR} cases were similar to the unusual profile reported by A13, the ULF implications of which are poorly understood.

3. Results

[16] We calculate power spectral densities of the (Hann windowed) components of the magnetic field for all events, with the median spectra shown in Figure 2a for high and low f_{FLR}, respectively. In both cases, power enhancements were observed in the poloidal and compressional components at frequencies in agreement with expected upstream waves f_{UW} generated in the ion foreshock [*Takahashi et al.*, 1984] (calculated using OMNI data for cone angles < 50° [*Le and Russell*, 1992]) which are known to be convected into the magnetosphere [e.g., *Clausen et al.*, 2009]. However, the magnetospheric response was otherwise different for the two f_{FLR} cases.

[17] For high f_{FLR}, i.e., GOES outside the plasmasphere, there is clear evidence of toroidal mode field line resonances at the harmonics of the most common FLR frequency (multiple peaks in B_A in agreement with the grey histogram). While there is no clear power enhancement at the fundamental frequency, they are expected to be weak near the equator [*Singer and Kivelson*, 1979]. In the compressional and poloidal components, broadband power increases (compared to the null events) predominantly at Pc5–6 frequencies were observed with additional enhancements at discrete frequencies (also observed in the toroidal mode) consistent with the magic frequencies of the magnetosphere. However, such discrete frequencies were not observed in the magnetosheath or solar wind (not shown) pressures, the former showing only broadband power increases against the null events. Thus, for these events, the magic frequencies were not, as proposed by *Kepko et al.* [2002] and *Kepko and Spence* [2003], present upstream.

[18] Time frequency analysis can better identify causal relations between the magnetosheath pressure and the waves observed in the magnetosphere, thus we Morlet wavelet transform [*Torrence and Compo*, 1998] the data and combine the wavelet power over events. The median dynamic spectra for $f_{\mathrm{FLR}} > 10$ mHz events are shown in Figure 2b that highlights time asymmetries before and after the jets. The compressional power before the jet is broadband and similar to the magnetosheath pressure at frequencies <2 mHz with higher frequencies being increasingly suppressed, consistent with the low-pass filtered directly driven response reported by A13. In contrast, after the jet, the results show discrete power enhancements (weaker than those previously) at some of the magic frequencies, even when there is little corresponding power in the magnetosheath pressure, e.g., the second magic frequency. The poloidal component contains power predominantly at magic frequencies both before and after the jet, implying radial motions at these frequencies. There is a clear shift to higher magic frequencies after

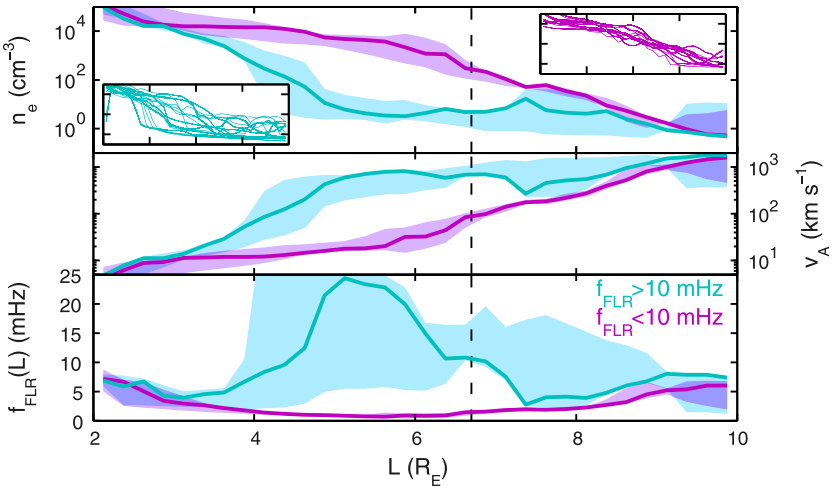

Figure 1. Median L shell profiles of (top) the magnetospheric electron number density, (middle) equatorial Alfvén speed, and (bottom) fundamental FLR frequency for the low (purple) and high (turquoise) FLR frequency cases. In the insets are the observations for all events in the same format. Shaded areas indicate the interquartile range and geostationary orbit is highlighted by the dashed line.

the jet which is also seen in the compressional component. Thus, the magnetospheric response is a combination of both directly driven and resonant waves. It should be noted that there was a slight biasing by events on 1 day in this case, though the supporting information shows that the results are qualitatively similar even when excluding this day.

[19] In the case of low f_{FLR}, magnetospheric wave power is significantly reduced (Figure 2a, bottom). This is in part due to less driving power in the magnetosheath pressure; however, this cannot fully account for the weak response, thus the steady density transition for these events (Figure 1) may be affecting ULF wave penetration. While it is beyond

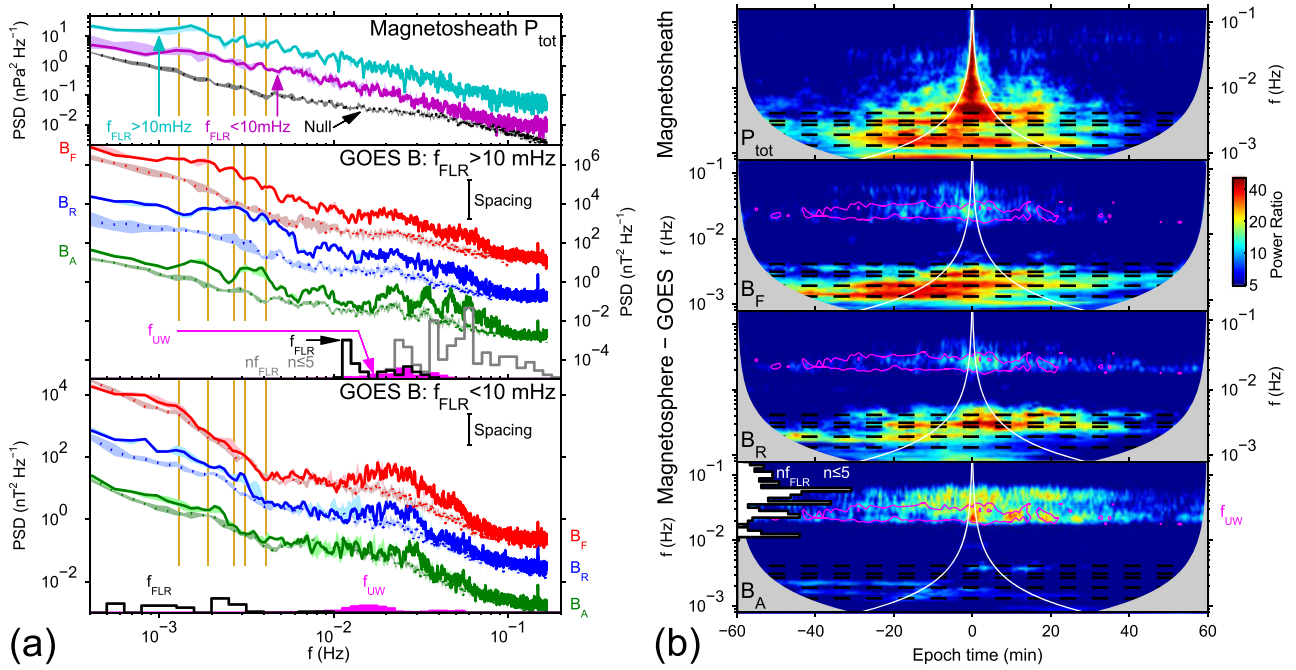

Figure 2. (a) Median power spectra of the (top) magnetosheath total pressure and magnetospheric magnetic field components for the (middle) high and (bottom) low FLR frequency cases along with their respective null spectra (dots). Note the different axis limits and spacing between components. Also shown is the distribution of expected upstream waves (magenta) and the fundamental (black) and harmonics (grey) of field line resonances. Shaded areas indicate the standard error and the magic frequencies of *Plaschke et al.* [2009] are shown as the vertical lines. (b) Median dynamic spectra for the high FLR frequency case. Power law fits to the null event spectra have been divided for clarity. The cone of influence centered on zero epoch is shown (white) along with the expected times and frequencies of upstream waves (magenta; 50% contour level) and the magic frequencies (black dashes).

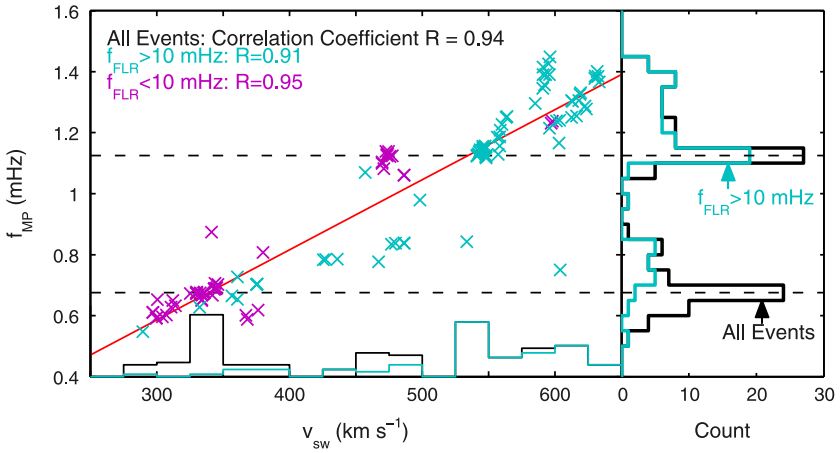

Figure 3. (left) Estimated fundamental magnetopause surface eigenmode frequencies as a function of solar wind speed (crosses) along with the distribution of the latter and a best fit line (red). (right) The distribution of estimated frequencies.

the scope of this study to fully address this topic, it should be noted that for Pc5 waves, the length scale of the density transition is much smaller than the perpendicular wavelength; hence, GOES is effectively inside the plasmasphere. Since it is known that Pc5 power is lower inside the plasmasphere compared to outside [e.g., *Hartinger et al.*, 2010], this reduced wave power is perhaps to be expected. Figure 2a (bottom) shows marginal power enhancements at magic frequencies observed in these cases, though these tend to be at lower ones than in the high f_{FLR} case. In fact there is very little power at frequencies greater than the largest f_{FLR}, consistent with A13 who suggested, under this unusual FLR frequency profile, compressional wave power converting to toroidal mode FLRs, would appear as a low-pass filtering effect with decreasing L shell. Indeed, there is evidence of fundamental toroidal mode FLRs with a small enhancement in power at the most common f_{FLR}. Interestingly, the median dynamic spectra (not shown) did not clearly display the shift to higher magic frequencies after the jet in this case.

4. Analysis

[20] We have shown that magic frequencies can be excited in the magnetosphere by broadband magnetosheath jets, thus for these events, they are likely eigenfrequencies of the magnetosphere. Here we distinguish between the two remaining hypotheses: global modes and magnetopause surface eigenmodes.

4.1. Global Modes

[21] We can estimate the expected fundamental frequency of global modes outside the plasmasphere using the time of flight approximation in the cold plasma limit. We do this only for events where the plasmapause was well defined and assume quarter wavelength modes, i.e., fixed at the plasmapause and open at the magnetopause. This yields fundamental frequencies between 10 and 40 mHz, consistent with previous results [*Lee and Lysak*, 1989; *Hartinger et al.*, 2013] and much higher than the observed magic frequencies. While compositional effects ignored in the estimation could reduce these values, they could not account for the factor of ~10 required.

[22] Further evidence against the global mode interpretation of the magic frequencies comes from multipoint observations. We identified events when in addition to GOES, one of the THEMIS spacecraft was in the outer magnetosphere within our MLT range. This was the case for 45 events, where the spacecraft was typically at L shells between ~8 and 9. Since the positions of the boundaries vary significantly over all events, both spacecraft sample varying fractional distances between them. However, the power observed by THEMIS at all of the magic frequencies was universally larger than at GOES, thus the wave amplitudes monotonically decreased with distance for all harmonics of the fundamental magic frequency. It is therefore unlikely that the magic frequencies can be explained as radially standing global modes, which should contain nodes and antinodes especially for higher harmonics. The observations are more likely explained as evanescent waves, as expected from the magnetopause surface eigenmode interpretation. Finally, the expected polarization for global modes [*Waters et al.*, 2002] was observed by THEMIS in only seven events (16%). Thus, the magic frequencies triggered by the magnetosheath jets are largely inconsistent with global modes.

4.2. Surface Eigenmodes

[23] The multipoint observations in the magnetosphere are consistent with an evanescent surface eigenmode interpretation of the magic frequencies; however, it is not clear why such stable eigenfrequencies exist over a wide range of upstream conditions. We therefore estimate the fundamental surface eigenmode frequency f_{MP} using a similar method to *Plaschke et al.* [2009]. The phase speed of an Alfvénic surface wave is given by [*Chen and Hasegawa*, 1974]

$$v = \sqrt{\frac{B_0^2 + B_1^2}{\mu_0(\rho_0 + \rho_1)}} \tag{1}$$

where 0 and 1 represent the magnetosphere and magnetosheath sides of the magnetopause boundary, respectively. We calculate the phase speed at the subsolar point for all events, setting the magnetosheath densities and fields as 3.6 and 4.2 times their respective solar wind values (from Block Adaptive Tree Solar Wind Roe Upwind Scheme

[*Powell et al.*, 1999]) with the magnetospheric field set by pressure balance and density assumed to be 1 cm^{-3}. Changing densities or fields by 10% affect the results by only ∼2%. The resulting phase speeds ranged ∼240–520 km s^{-1} and were highly correlated with the solar wind speed (R = 0.995). We also calculate the length of the magnetopause field lines from the T96 model which ranged ∼25–40 R_E. Assuming a constant phase speed along the field lines, we arrive at estimates of f_{MP} for all events shown in Figure 3 (left), which were also highly correlated to the solar wind speed.

[24] Since the solar wind speed has a bimodal distribution (Figure 3, bottom histogram), corresponding to slow and fast wind, so too does the distribution of f_{MP}. These two populations (black histogram) have surprisingly well-defined preferential frequencies (standard deviations ∼0.1 mHz). For slow wind, this is 0.7 mHz, in excellent agreement with the fundamental magic frequency reported in the literature and also consistent with the estimation of *Plaschke et al.* [2009]. The results show a higher fundamental frequency is expected for fast wind, with our estimates giving a value of 1.15 mHz which may be consistent with the 1.3 mHz magic frequency previously reported. Therefore, we demonstrate for the first time that even with a wide range of upstream conditions (further discussion in the supporting information), the magnetopause surface wave theory yields preferential frequencies, correlated to the solar wind speed, consistent with the magic frequencies of the magnetosphere. Further work, using for instance ground magnetometers, could test this predicted correlation of geomagnetic pulsation frequencies with solar wind speed.

[25] Figure 3 (right) also shows the distribution of surface wave frequencies for the high f_{FLR} events, revealing these to be dominated by fast solar wind and thus higher magic frequencies, consistent with the observations in the magnetosphere. Furthermore, the shift in magic frequencies after the jet seen in the dynamic spectra (Figure 2b) might be explained by the sharpest features of the jets locally perturbing the boundary [e.g., *Shue et al.*, 2009] thus resonantly exciting harmonics of the surface eigenmodes, in contrast to the quasi-static/filtered driving at low frequencies before the jet (A13).

5. Conclusion

[26] In this paper we have shown that, in the absence of monochromatic fluctuations upstream, broadband jets in the subsolar magnetosheath directly and resonantly drive ULF waves in the magnetosphere at the so-called magic frequencies, as well as local field line resonances. Under unusual steady density transitions between the plasmasphere and outer magnetosphere, the penetration of these waves appears to be reduced however. We have shown that even under a wide range of upstream conditions, the expected fundamental frequencies of standing Alfvénic magnetopause surface waves are highly correlated to the solar wind speed yielding two preferential values, corresponding to slow and fast wind, and that the harmonics of these are in good agreement with the magic frequencies. In contrast, the expected frequencies of global modes outside the plasmasphere are too high and multipoint and polarization measurements show the magic frequencies are not consistent with this, often assumed, interpretation. Thus, we conclude that the magic frequencies triggered by the jets are most likely magnetopause surface eigenmodes.

[27] **Acknowledgments.** We thank one of the reviewers for the thorough and diligent comments. This research at Imperial College London was funded by STFC grant ST/I505713/1. M.D. Hartinger was funded through NSF grant AGS-1230398. We acknowledge NASA contract NAS5-02099 and V. Angelopoulos for use of data from the THEMIS mission, specifically, C. W. Carlson and J. P. McFadden for use of ESA data; J. W. Bonnell and F. S. Mozer for use of EFI data; and K. H. Glassmeier, U. Auster, and W. Baumjohann for use of FGM data provided under the lead of the Technical University of Braunschweig and with financial support through the German Ministry for Economy and Technology and the German Center for Aviation and Space (DLR) under contract 50 OC 0302. For GOES magnetometer data, we thank H. J. Singer. The OMNI data were obtained from the NASA/GSFC OMNIWeb interface at http://omniweb.gsfc.nasa.gov.

[28] The Editor thanks two anonymous reviewers for their assistance in evaluating this paper.

References

Angelopoulos, V. (2008), The THEMIS mission, *Space Sci. Rev.*, *141*, 5–34, doi:10.1007/s11214-008-9336-1.

Archer, M. O., and T. S. Horbury (2013), Magnetosheath dynamic pressure enhancements: Occurrence and typical properties, *Ann. Geophys.*, *31*, 319–331, doi:10.5194/angeo-31-319-2013.

Archer, M. O., T. S. Horbury, and J. P. Eastwood (2012), Magnetosheath pressure pulses: Generation downstream of the bow shock from solar wind discontinuities, *J. Geophys. Res.*, *117*, A05228, doi:10.1029/2011JA017468.

Archer, M. O., T. S. Horbury, J. P. Eastwood, J. M. Weygand, and T. K. Yeoman (2013), Magnetospheric response to magnetosheath pressure pulses: A low pass filter effect, *J. Geophys. Res. Space Physics*, *118*, doi:10.1002/jgra.50519.

Auster, H. U., et al. (2008), The THEMIS fluxgate magnetometer, *Space Sci. Rev.*, *141*, 235–264, doi:10.1007/s11214-008-9365-9.

Chen, L., and A. Hasegawa (1974), A theory of long-period magnetic pulsations: 2. Impulse excitation of surface eigenmode, *J. Geophys. Res.*, *79*, 1033–1037, doi:10.1029/JA079i007p01033.

Clausen, L. B. N., T. K. Yeoman, R. C. Fear, R. Behlke, E. A. Lucek, and M. J. Engebretson (2009), First simultaneous measurements of waves generated at the bow shock in the solar wind, the magnetosphere and on the ground, *Ann. Geophys.*, *27*, 357–371, doi:10.5194/angeo-27-357-2009.

Francia, P., and U. Villante (1997), Some evidence of ground power enhancements at frequencies of global magnetospheric modes at low latitude, *Ann. Geophys.*, *15*, 17–23, doi:10.1007/s00585-997-0017-2.

Hartinger, M., M. B. Moldwin, V. Angelopoulos, K. Takahashi, H. J. Singer, R. R. Anderson, Y. Nishimura, and J. R. Wygant (2010), Pc5 wave power in the quiet-time plasmasphere and trough: CRRES observations, *Geophys. Res. Lett.*, *37*, L07107, doi:10.1029/2010GL042475.

Hartinger, M. D., V. Angelopoulos, M. B. Moldwin, K. Takahashi, and L. B. N. Clausen (2013), Statistical study of global modes outside the plasmasphere, *J. Geophys. Res. Space Physics*, *118*, 804–822, doi:10.1002/jgra.50140.

Kepko, L., and H. E. Spence (2003), Observations of discrete, global magnetospheric oscillations directly driven by solar wind density variations, *J. Geophys. Res.*, *108*, 1257, doi:10.1029/2002JA009676.

Kepko, L., H. E. Spence, and H. J. Singer (2002), ULF waves in the solar wind as direct drivers of magnetospheric pulsations, *Geophys. Res. Lett.*, *29*, 1197, doi:10.1029/2001GL014405.

Kivelson, M. G., and D. J. Southwood (1985), Resonant ULF waves: A new interpretation, *Geophys. Res. Lett.*, *12*, 49–52, doi:10.1029/GL012i001p00049.

Le, G., and C. T. Russell (1992), A study of ULF wave morphology—I: ULF foreshock boundary, *Planet. Space Sci.*, *40*, 1203–1213, doi:10.1016/0032-0633(92)90077-2.

Lee, D.-H., and R. L. Lysak (1989), Magnetospheric ULF wave coupling in the dipole model: The impulsive excitation, *J. Geophys. Res.*, *94*, 17,097–17,103, doi:10.1029/JA094iA12p17097.

McFadden, J. P., C. W. Carlson, D. Larson, M. Ludlam, R. Abiad, B. Elliott, P. Turin, M. Marckwordt, and V. Angelopoulos (2008a), The THEMIS ESA plasma instrument and in-flight calibration, *Space Sci. Rev.*, *141*, 277–302, doi:10.1007/s11214-008-9440-2.

McFadden, J. P., C. W. Carlson, J. Bonnell, F. Mozer, V. Angelopoulos, K. H. Glassmeier, and U. Auster (2008b), THEMIS ESA first science results and performance issues, *Space Sci. Rev.*, *141*, 447–508, doi:10.1007/s11214-008-9433-1.

Menk, F. W. (2011), Magnetospheric ULF waves: A review, in *The Dynamic Magnetosphere*, edited by W. Lui and M. Fujimoto,

pp. 223–256, IAGA Special Sopron Book Series, Springer-Verlag Berlin, Dordrecht, The Netherlands, doi:10.1007/978-94-007-0501-2_13.

Plaschke, F., and K. H. Glassmeier (2011), Properties of standing Kruskal-Schwarzschild-modes at the magnetopause, *Ann. Geophys.*, *29*, 1793–1807, doi:10.5194/angeo-29-1793-2011.

Plaschke, F., K.-H. Glassmeier, H. U. Auster, O. D. Constantinescu, W. Magnes, V. Angelopoulos, D. G. Sibeck, and J. P. McFadden (2009), Standing Alfvén waves at the magnetopause, *Geophys. Res. Lett.*, *36*, L02104, doi:10.1029/2008GL036411.

Powell, K. G., P. L. Roe, T. J. Linde, T. I. Gombosi, and D. L. De Zeeuw (1999), A solution-adaptive upwind scheme for ideal magnetohydrodynamics, *J. Comput. Phys.*, *154*, 284–309, doi:10.1006/jcph.1999.6299.

Samson, J. C., B. G. Harrold, J. M. Ruohoniemi, R. A. Greenwald, and A. D. M. Walker (1992), Field line resonances associated with MHD wave guides in the magnetosphere, *Geophys. Res. Lett.*, *19*, 441–444, doi:10.1029/92GL00116.

Shue, J.-H., J.-K. Chao, P. Song, J. P. McFadden, A. Suvorova, V. Angelopoulos, K. H. Glassmeier, and F. Plaschke (2009), Anomalous magnetosheath flows and distorted subsolar magnetopause for radial interplanetary magnetic fields, *Geophys. Res. Lett.*, *36*, L18112, doi:10.1029/2009GL039842.

Singer, H. J., and M. G. Kivelson (1979), The latitudinal structure of Pc5 waves in space: Magnetic and electric field observations, *J. Geophys. Res.*, *84*, 7213–7222, doi:10.1029/JA084iA12p07213.

Southwood, D. J. (1974), Some features of field line resonances in the magnetosphere, *Planet. Space Sci.*, *22*, 483–491, doi:10.1016/0032-0633(74)90078-6.

Takahashi, K., R. L. McPherron, and T. Terasawa (1984), Dependence of the spectrum of Pc 3–4 pulsations on the interplanetary magnetic field, *J. Geophys. Res.*, *89*, 2770–2780, doi:10.1029/JA089iA05p02770.

Torrence, C., and G. P. Compo (1998), A practical guide to wavelet analysis, *Bull. Amer. Meteor. Soc.*, *79*, 61–78, doi:10.1175/1520-0477(1998)079<0061:APGTWA>2.0.CO;2.

Tsyganenko, N. A. (1995), Modeling the Earth's magnetospheric magnetic field confined within a realistic magnetopause, *J. Geophys. Res.*, *100*, 5599–5612, doi:10.1029/94JA03193.

Tsyganenko, N. A., and D. P. Stern (1996), Modeling the global magnetic field of the large-scale Birkeland current systems, *J. Geophys. Res.*, *101*, 27,187–27,198, doi:10.1029/96JA02735.

Tu, J., P. Song, B. W. Reinisch, and J. L. Green (2007), Smooth electron density transition from plasmasphere to the subauroral region, *J. Geophys. Res.*, *112*, A05227, doi:10.1029/2007JA012298.

Viall, N. M., L. Kepko, and H. E. Spence (2009), Relative occurrence rates and connection of discrete frequency oscillations in the solar wind density and dayside magnetosphere, *J. Geophys. Res.*, *114*, A01201, doi:10.1029/2008JA013334.

Waters, C. L., K. Takahashi, D.-H. Lee, and B. J. Anderson (2002), Detection of ultralow-frequency cavity modes using spacecraft data, *J. Geophys. Res.*, *107*, 1284, doi:10.1029/2001JA000224.